

# Alfvén Wave Amplification and Self-Containment of Cosmic-Rays Escaping from a Supernova Remnant

Yutaka Fujita<sup>1\*</sup>, Fumio Takahara<sup>1</sup>, Yutaka Ohira<sup>2</sup>, and Kazunari Iwasaki<sup>3</sup>

<sup>1</sup>*Department of Earth and Space Science, Graduate School of Science, Osaka University,*

*1-1 Machikaneyama-cho, Toyonaka, Osaka 560-0043, Japan*

<sup>2</sup>*Theory Centre, Institute of Particle and Nuclear Studies, KEK, 1-1 Oho, Tsukuba 305-0801, Japan*

<sup>3</sup>*Department of Physics, Nagoya University, Nagoya 464-8602, Japan*

Accepted 0000 December 00. Received 0000 December 00; in original form 0000 October 00

## ABSTRACT

We study the escape of cosmic-ray (CR) protons accelerated at a supernova remnant (SNR) by numerically solving a diffusion-convection equation from the vicinity of the shock front to the region far away from the front. We consider the amplifications of Alfvén waves generated by the escaping CR particles and their effects on CR escape into interstellar medium (ISM). We find that the amplification of the waves significantly delays the escape of the particles even far away from the shock front (on a scale of the SNR). This means that the energy spectrum of CR particles measured through  $\gamma$ -ray observations at molecular clouds around SNRs is seriously affected by the particle scattering by the waves.

**Key words:** ISM: clouds – cosmic rays – ISM: supernova remnants

## 1 INTRODUCTION

Cosmic rays (CRs) are relativistic charged particles and most of them are believed to be accelerated at the shock front of supernova remnants (SNRs). In fact, TeV  $\gamma$ -ray emissions have been detected with H.E.S.S. from the shell of young SNRs (Aharonian et al. 2004, 2005). Moreover, GeV  $\gamma$ -ray emissions have been detected with Fermi and AGILE from middle-aged SNRs surrounded by molecular clouds. They are likely to be generated via a hadronic process, i.e. inelastic collisions between CR protons accelerated at SNRs and ambient protons (Abdo et al. 2009, 2010a,b,c; Tavani et al. 2010; Giuliani et al. 2010). TeV  $\gamma$ -ray emissions have also been discovered from some of these clouds (Aharonian et al. 2008). The energy spectrum of CR protons is not described by a single power-law. Thus, it is most likely to be affected by an escape process from SNR shocks (but see also Uchiyama et al. 2010).

The  $\gamma$ -ray observations of molecular clouds around SNRs have given us information not only on the CR particle acceleration in the SNRs but also on the escape of the particles from the SNRs (e.g. Ptuskin & Zirakashvili 2003; Caprioli, Blasi, & Amato 2009; Ohira, Murase, & Yamazaki 2010; Kawanaka et al. 2011; Ohira, Murase, & Yamazaki 2011). In particular, their escape into the surrounding interstellar medium (ISM) is important to compare the  $\gamma$ -ray observations of

molecular clouds around the SNRs with theoretical models of particle acceleration. Recently, Lee, Kamae, & Ellison (2008) and Gabici, Aharonian, & Casanova (2009) theoretically studied the escape into the ISM and obtained an energy spectrum of the escaped particles. In their studies, they assumed that the diffusion coefficient for the particle diffusion outside the SNR is the one in the general region in the Galaxy. However, Fujita et al. (2009) suggested that the observations seem to show that the diffusion time-scale of CRs around SNRs is much longer than that in the general region in the Galaxy. They estimated that the diffusion coefficient must be less than  $\sim 1\%$  of that in the general region to be consistent with the observations of the SNR W 28 and another possible SNR in Westerlund 2 (see also Torres, Rodríguez Marrero, & de Cea Del Pozo 2008). Motivated by these results, Fujita, Ohira, & Takahara (2010) theoretically studied the diffusion of particles in ISM after they left the shock neighbourhood. They used Monte-Carlo simulations to follow a particle motion, while at the same time they calculated the evolution of the SNR. They considered the excitation of Alfvén waves through the streaming instability caused by CRs, and the interactions between the waves and the particles. Since the growth of the waves changes the diffusion coefficient, they took the evolution of the diffusion coefficient into consideration. They found that the particles actually excite Alfvén waves around the SNR on a spatial scale of the SNR itself if the ISM is highly ionised. Thus, even if the particles can leave the shock neighbourhood, scattering by the waves prevents

\* E-mail: fujita@vega.ess.sci.osaka-u.ac.jp (YF)

them from moving further away from the SNR. This means that the particles cannot virtually escape from the SNR until a fairly late stage of the SNR evolution.

However, the model developed by Fujita, Ohira, & Takahara (2010) may still be rather simplified. In particular, they separately treated the acceleration of particles at the shock front and their propagation into the surrounding ISM. Since both of the processes follow the same transport equation, they should be treated seamlessly. In this paper, we present the results of our numerical simulations that deal with both the particle acceleration and the diffusion into the ISM at the same time. In these simulations, we take account of the streaming instability developed by the flux of CRs in order to study how the growth of the Alfvén waves affects the diffusion of the CRs. We emphasise that we focus on the propagation of CRs far away from the shock front ( $r - R_s \sim R_s$ , where  $r$  is the distance from the SNR centre and  $R_s$  is the shock radius), in contrast with previous studies that treat the escape around the shock front ( $r - R_s \ll R_s$ ; e.g. Vladimirov, Ellison, & Bykov 2006). As far as we know, this is the first time to solve a transport equation from the shock vicinity to the region far away from the shock front.

## 2 MODELS

### 2.1 Equations

The diffusion of CR particles obeys the transport equation (diffusion-convection equation):

$$\frac{\partial f}{\partial t} = \nabla(\kappa \nabla f) - \mathbf{w} \nabla f + \frac{\nabla \mathbf{w}}{3} p \frac{\partial f}{\partial p} + Q, \quad (1)$$

where  $f(r, p, t)$  is the distribution function of the particles,  $p$  is the momentum,  $\kappa$  is the diffusion coefficient,  $\mathbf{w}$  is the hydrodynamic velocity of the background gas, and  $Q = Q_0 \delta(r - R_s)$  is the source term for the particles, which are injected at the shock front ( $r = R_s$ ) at a momentum of  $p_{\text{inj}}$ . The coefficient  $Q_0$  is given by

$$Q_0 = \epsilon \frac{\rho_1 u_1}{m} \frac{\delta(p - p_{\text{inj}})}{4\pi p_{\text{inj}}^2}, \quad (2)$$

where  $\rho_1$  and  $u_1$  are the gas density and the gas velocity relative to the shock just upstream the shock front, respectively. In § 3, we set  $p_{\text{inj}} = 2 m c_{s2}$ , where  $c_{s2}$  is the sound velocity behind the shock front. The fraction of gas particles that go into the acceleration process at the shock front is  $\epsilon = 10^{-4}$ .

The equations for the background gas are

$$\frac{\partial \rho}{\partial t} + \nabla(\rho \mathbf{w}) = 0, \quad (3)$$

$$\rho \frac{\partial \mathbf{w}}{\partial t} + \rho(\mathbf{w} \cdot \nabla) \mathbf{w} = -\nabla(P_c + P_g), \quad (4)$$

$$\frac{\partial P_g}{\partial t} + (\mathbf{w} \cdot \nabla) P_g + \gamma_g (\nabla \mathbf{w}) P_g = 0, \quad (5)$$

where  $\rho$ ,  $\gamma_g$ , and  $P_g$  are the density, specific heat capacity ratio, and pressure of the gas. The CR pressure is given by

$$P_c = \frac{4\pi c}{3} \int_{p_{\text{min}}}^{\infty} dp \frac{p^4 f}{\sqrt{p^2 + m^2 c^2}}, \quad (6)$$

where  $p_{\text{min}}$  is the minimum momentum of injected CR particles,  $m$  is the mass of the particles, and  $c$  is the velocity of light. We consider only protons and neglect electrons.

### 2.2 Diffusion Coefficient and Initial Conditions

Since we treat the propagation of CRs away from the shock front, we cannot assume a plane geometry. Therefore, we assume spherical symmetry and solve equations (1)–(5) mainly based on the numerical methods developed by Berezhko, Yelshin, & Ksenofontov (1994). We do not fix the diffusion coefficient  $\kappa$  at the value corresponding to the Bohm diffusion, which is different from the studies by Berezhko, Yelshin, & Ksenofontov (1994). Instead, we follow the evolution of  $\kappa$  in this study, considering the amplification of Alfvén waves by CR particles. Since the waves scatter the particles, they affect the diffusion coefficient in equation (1). The growth of the waves is given by

$$\frac{\partial \psi}{\partial t} \approx \frac{4\pi}{3} \frac{v_A p^4 v}{U_M} |\nabla f|, \quad (7)$$

where  $\psi(t, \mathbf{r}, p)$  is the energy density of Alfvén waves per unit logarithmic bandwidth (which are resonant with particles of momentum  $p$ ) relative to the ambient magnetic energy density  $U_M$ , and  $v_A$  is the Alfvén velocity (Skilling 1975; Bell 1978). We do not consider the damping of the waves for simplicity. The diffusion coefficient is

$$\kappa = \frac{4}{3\pi} \frac{p v c}{e B_0 \psi} \frac{\rho_0}{\rho}, \quad (8)$$

where  $v$  is the velocity of the particle,  $e$  is the elementary charge,  $B_0$  is the unperturbed magnetic field, and  $\rho_0$  is the density of unperturbed ISM. Following Berezhko, Yelshin, & Ksenofontov (1994), we included the influence of gas compression on the magnetic field ( $B = B_0 \rho / \rho_0$ ) and particle scattering by assuming that  $\kappa$  depends on the gas density.

The diffusion coefficient corresponding to the Bohm diffusion is given by  $\kappa_{B0} = \rho_B c / 3$ , where  $\rho_B = pc / (e B_0)$  is the gyroradius of particles. We calculate the evolution of the gas and CR particles using the methods of Berezhko, Yelshin, & Ksenofontov (1994) for  $r \lesssim r_b(p) \equiv 4\kappa_{B0} / V_s + R_s$  and  $p / (mc) \gtrsim 10^{-3.4}$ , where  $V_s$  is the shock velocity. We call this region the “shock region”. Since we are also interested in the CR diffusion outside this region, we added equal interval meshes for  $r_b(p) \lesssim r \lesssim r_{\text{out}}(p) \equiv 500 \kappa_{B0} / V_s + r_b$ . We call this surrounding region the “escape region”. For this region, we calculate the diffusion of the CR particles only with  $p / (mc) \gtrsim 10^{2.4}$ . For this energy range, the escape region is sufficiently apart from the shock front, and the feedback of the CR particles on hydrodynamics is small there. Thus, we ignore the feedback in this region ( $\nabla \mathbf{w} \sim 0$ ) and solve equation (1) without considering the change of  $f$  in the direction  $p$  (the third term in the right hand of equation [1]), which makes calculations much easier. The term  $\mathbf{w} \nabla f$  in equation (1) can also be ignored in this region, although we do not omit the term in the calculations. On the other hand, we do not solve the diffusion of particles with  $p / (mc) \lesssim 10^{2.4}$  in the escape region, because  $\nabla \mathbf{w}$  cannot be ignored even in the region. Since the feedback of the low-energy particles on hydrodynamics is limited in the

vicinity of the shock, they do not affect the following results at  $r - R_s \sim R_s$ . We set  $f = 0$  at  $r = r_{\text{out}}$ .

The initial condition of  $\psi$  is given as follows. The diffusion coefficient of the background ISM is given by

$$\kappa_{\text{ISM}} = 10^{28} \text{ cm}^2 \text{ s}^{-1} \left( \frac{E}{10 \text{ GeV}} \right)^{0.5} \left( \frac{B_0}{3 \mu\text{G}} \right)^{-0.5}, \quad (9)$$

where  $E$  is the particle energy (Gabici, Aharonian, & Casanova 2009). We relate  $\kappa_{\text{ISM}}$  to the energy density of Alfvén waves ( $\psi_{\text{ISM}}$ ):

$$\kappa_{\text{ISM}} = \frac{4}{3\pi} \frac{pvc}{eB_0\psi_{\text{ISM}}}. \quad (10)$$

If we set  $\psi = \psi_{\text{ISM}}$  at  $t = t_{\text{inj}}$ , where  $t_{\text{inj}}$  is the time when we start injecting CRs,  $\psi$  does not grow enough and particles are not accelerated. As has been well known, for diffusive shock acceleration to work,  $\psi$  must be as large as that for Bohm diffusion near the shock front (e.g. Bell 1978; Lucek & Bell 2000). Thus, in this study, we simply assume that the diffusion at the shock front can be represented by Bohm diffusion ( $\kappa = \kappa_{\text{B0}}\rho_0/\rho$ ). One can find that the energy density of Alfvén waves corresponding to  $\kappa_{\text{B0}}$  is  $\psi_{\text{B}} = 4v/(\pi c) \approx 4/\pi$ . On the other hand, for  $r - R_s \gg \kappa_{\text{B0}}/V_s$ , the coefficient should be the one at the interstellar space ( $\kappa_0 = \kappa_{\text{ISM}}$ ). As the initial condition of  $\psi$  at  $t = t_{\text{inj}}$ , we interpolate the two  $\psi$ s:

$$\begin{aligned} \psi_i(r, p) &= (\psi_{\text{B}} - \psi_{\text{ISM}}) \exp \left[ -\frac{(r - R_s(t_{\text{inj}}))V_s(t_{\text{inj}})}{a_i \kappa_{\text{B0}}} \right] \\ &+ \psi_{\text{ISM}}, \end{aligned} \quad (11)$$

where  $a_i$  is a parameter. Although the value of  $a_i$  cannot be specified, it would not be much larger than one. Therefore we assume  $a_i = 5$  in the following simulations. The larger  $a_i$  gives the smaller diffusion coefficient at a given  $r$  and results in less escape of the particles. For values of  $a_i$  as small as one, it is increasingly difficult to obtain stable and precise results, because  $f$  changes rapidly at the boundary between the shock and escape region, where resolution is not high enough. We consider three models: (A) the growth of  $\psi$  is considered, (B) the diffusion coefficient is fixed at  $\kappa = \kappa_{\text{B0}}\rho_0/\rho$  regardless of time and position, and (C) the wave energy density does not change and is fixed at  $\psi = \psi_i$ , replacing  $t_{\text{inj}}$  with  $t$  in equation (11). The models B and C are calculated for comparison. In Model A, we set a lower limit of  $\psi$  as  $\psi \geq \psi_i$ , replacing  $t_{\text{inj}}$  with  $t$  in equation (11). Moreover, we set an upper limit of  $\psi$  as  $\psi \leq \psi_{\text{B}}$ .

Since we do not consider the neutral damping of the waves, we choose the ISM with a relatively high temperature. The density and sound velocity of the background ISM is  $\rho_0 = 7.0 \times 10^{-27} \text{ g cm}^{-3}$  and  $c_s = 154 \text{ km s}^{-1}$ , respectively. A supernova explodes at  $t = 0$  and  $r = 0$  with an energy of  $10^{51} \text{ erg}$ . The background magnetic field is  $B_0 = \sqrt{8\pi U_M} = 3 \mu\text{G}$ . We inject CR particles and calculate the growth of Alfvén waves (equation [7]) for  $t > t_{\text{inj}} = 0.55 t_0$ , where  $t_0$  is the time when the free expansion phase of the SNR ends and the Sedov phase begins. For the parameters we adopted,  $t_0 = 4.7 \times 10^3 \text{ yr}$ .

### 3 RESULTS AND DISCUSSION

In Figure 1a, we show the profiles of  $\psi$  at  $t = 10 t_0$  for Models A and C. At this time, the radius of the SNR is  $R_s = 73 \text{ pc}$ , and the compression ratio of the gas is  $\rho_2/\rho_0 = 3.6$ , where  $\rho_2$  is the gas density behind the shock, for Models A, B, and C. The left ends of the curves correspond to  $\psi_{\text{B}}$ , and the right ends correspond to  $\psi_{\text{ISM}}$ . The difference between Model A and C indicates that CR particles can significantly amplify Alfvén waves. In particular, the amplification occurs even in the region far away from the shock front (say, at  $r \sim 2 R_s$ ) for particles with  $pc = 20 \text{ TeV}$ . The profiles are given by the balance between the growth through streaming instability and the flow of low- $\psi$  gas from upstream on the shock coordinate. The amplification of the waves prohibits the diffusion of particles. In Figure 1b, we show the profiles of  $f$  at  $10 t_0$ . While the particles are confined around the shock front in Model B, they can extend to the region where  $\psi \sim \psi_{\text{ISM}}$  in Model C (Figure 1). The results when the growth of  $\psi$  is considered (Model A) are located between those two models, although the profiles of  $\psi$  and  $f$  are somewhat different between  $pc = 1$  and  $20 \text{ TeV}$  (Figure 1). The overall features of  $\psi$  and  $f$  do not change for  $t \gtrsim t_0$ .

The results for Model A can be explained as follows. Figure 2 shows the evolution of  $\psi$  and  $f$  for Model A for  $t_{\text{inj}} < t \leq t_0$ , normalised by  $R_s(t)$  in the radial direction. The radius of the SNR at  $t = t_0$  is  $R_s = 23 \text{ pc}$ . For  $pc = 1 \text{ TeV}$ ,  $\psi$  increases in the “instep” or the region where the gradient of  $\psi$  is small ( $0.02 \lesssim (r - R_s)/R_s \lesssim 2$ ). This is because of the leak of particles into the low- $\psi$  region ( $\psi \sim \psi_{\text{ISM}}$ ). On the other hand, for  $pc = 20 \text{ TeV}$ ,  $\psi$  increases in the “shin” or the region where the gradient of  $\psi$  is large ( $0.1 \lesssim (r - R_s)/R_s \lesssim 0.6$ ). The leak of particles into the low- $\psi$  region ( $\psi \sim \psi_{\text{ISM}}$ ) is less significant for  $pc = 20 \text{ TeV}$  than for  $pc = 1 \text{ TeV}$  (Figure 2b). This is because  $\psi_{\text{ISM}}$  at  $pc = 1 \text{ TeV}$  is smaller than that at  $pc = 20 \text{ TeV}$  (Figure 2a and equations 9 and 10). For smaller  $\psi_{\text{ISM}}$ , particles tend to go farther away from the shock front, if the distance is represented in the units of  $\kappa_{\text{B0}}/V_s$ . Thus, for  $pc = 1 \text{ TeV}$ , particles escaping into the instep make the gradient of  $f$  in the instep, while for  $pc = 20 \text{ TeV}$  most particles are confined in the shin and make the gradient of  $f$  in the shin. The gradient of  $f$  increases  $\psi$  (equation [7]).

CR particles that escape from an SNR illuminate molecular clouds around the SNR and could be observed in  $\gamma$ -rays through pion production. Figure 3 shows the spectra of particles at  $r = 1.1 R_s$  and  $2 R_s$  at  $t = 10 t_0$ . In Model B, only particles with high energies can reach  $r \sim 1.1 R_s$ , because the diffusion coefficient for low-energy particles is small. On the other hand, in Models A and C, even low-energy particles can reach this radius, and the trend is more prominent at larger radii ( $r \sim 2 R_s$ ). Comparison between Models A and C shows that the effect of the wave growth cannot be ignored in the region away from the shock front ( $r = 2 R_s$ ); the energy density of particles at  $p/mc \sim 10^{4.5}$  in Model A is smaller than that in Model C by more than a factor of 10. In Figure 3, the broad hump of  $p^4 f$  at  $p/mc \sim 10^{3.5}$  at  $r \sim 2 R_s$  for Models A and C reflects the escape of particles into the instep region of  $\psi \sim \psi_{\text{ISM}}$  shown in Figure 1 for  $pc = 1 \text{ TeV}$ . The dip at  $p/mc \sim 10^{4.5}$  at  $r \sim 2 R_s$  for Model A is made because the particles hardly reach that

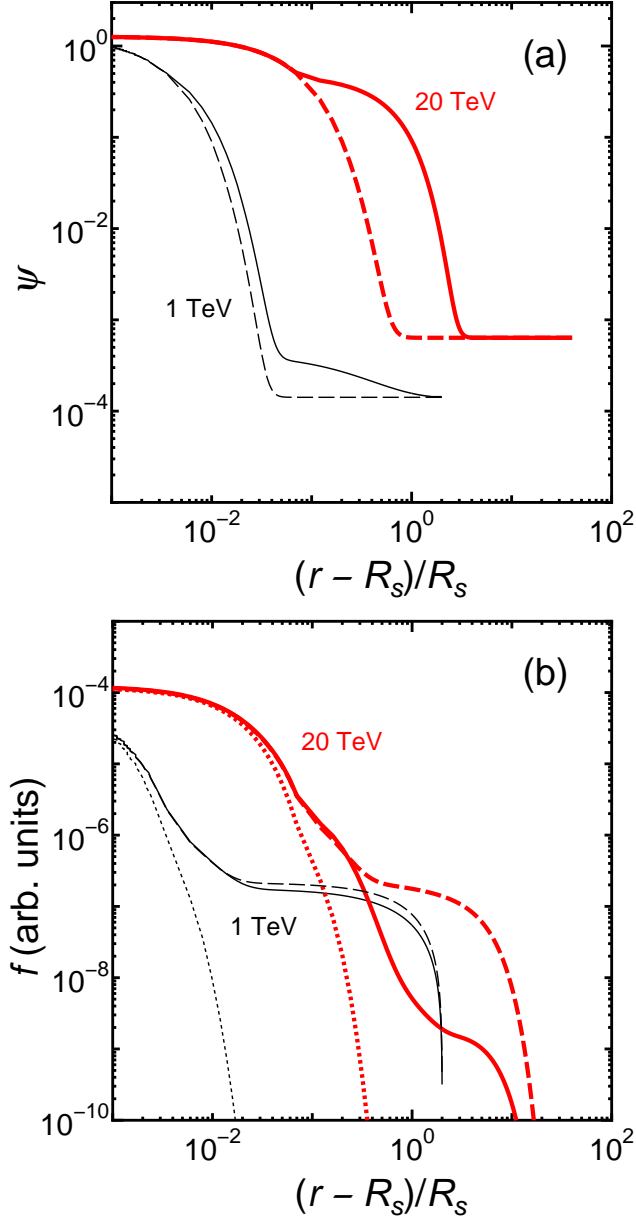


**Figure 1.** Profiles of wave energy density  $\psi$  at  $t = 10 t_0$ . Thin lines correspond to waves interacting with particles with  $pc = 1$  TeV and thick lines correspond to those with  $pc = 20$  TeV. Solid lines are for Model A and dashed lines are for Model C. (b) Same as (a) but for CR distribution  $f$ .

radius because of the growth of  $\psi$  in the shin ( $pc = 20$  TeV in Figure 1). The peaks at  $p/mc \sim 10^{5.3}$  for Models A, B and C mean that the region of  $\psi \sim \psi_B$  and the particles confined in that region reach  $r \sim 2 R_s$  and those particles are freely escaping in our treatment effectively. The decrease of spectra for Models A and C at  $r = 2 R_s$  for  $p/mc \lesssim 10^{3.5}$  suggests that the spectra are affected by the outer boundary condition of  $f = 0$ , because  $r_{\text{out}}(p)$  is relatively close to  $2 R_s$ . If  $r_{\text{out}}(p)$  is set at a larger radius, we expect that more particles reach  $r \gtrsim 2 R_s$ .

At  $t = 10 t_0$ , the total energies of CRs for  $r > 2 R_s$  are  $4.0 \times 10^{48}$ ,  $2.3 \times 10^{47}$ , and  $3.0 \times 10^{49}$  erg for Models A, B and C, respectively. These results show that the growth

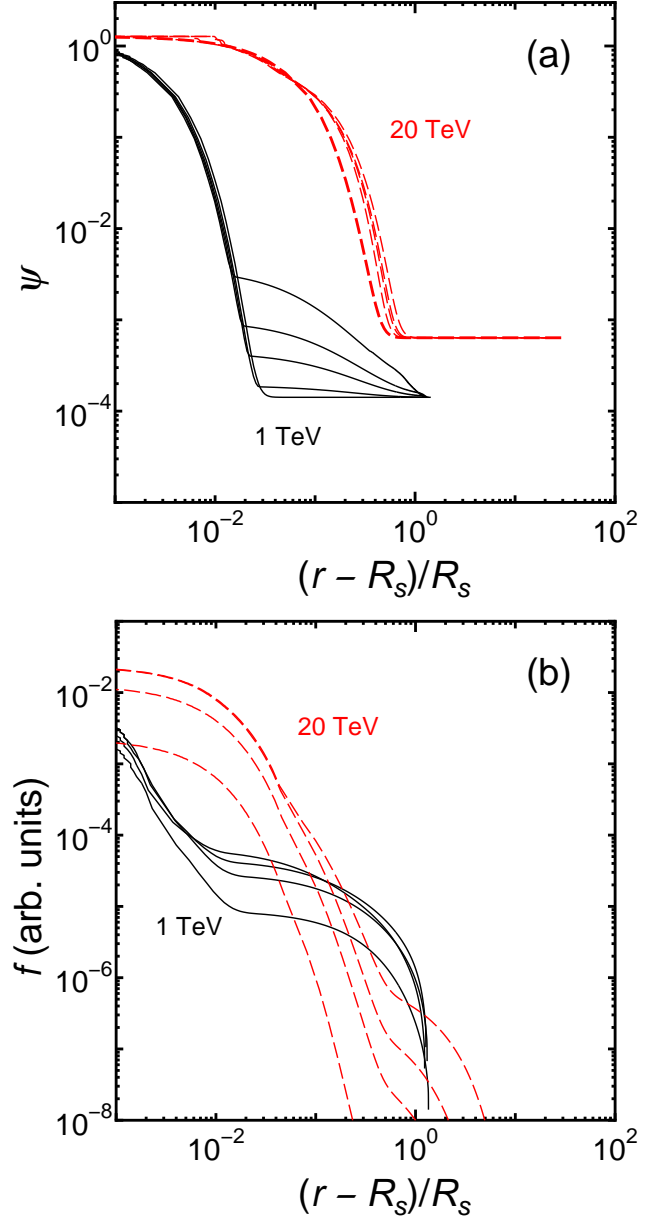


**Figure 2.** (a) Profiles of wave energy density  $\psi$  for Model A at  $t = 0.55 t_0$ ,  $0.60 t_0$ ,  $0.65 t_0$ ,  $0.70 t_0$ , and  $1.0 t_0$  (from bottom to top). (b) Same as (a) but for CR distribution  $f$  at  $t = 0.60 t_0$ ,  $0.65 t_0$ ,  $0.70 t_0$ , and  $1.0 t_0$  (from bottom to top).

of the waves can significantly change the CR spectrum and density around a middle-aged SNR, which should affect the  $\gamma$ -ray emission originated from the CRs. In this study, we did not treat particles with  $pc \sim \text{GeV}$ . However, above discussion suggests that many of them can escape into the instep region, because  $\psi_{\text{ISM}}$  for these energies are fairly small. It is to be noted that the results shown here do not involve the effect of wave damping. For example, if the ISM is not fully ionised, the Alfvén waves may damp through collisions between charged and neutral particles (Kulsrud & Cesarsky 1971; O’C Drury, Duffy, & Kirk 1996). If this happens, the spectrum of the escaped CR particles would be significantly changed (Fujita, Ohira, & Takahara 2010).

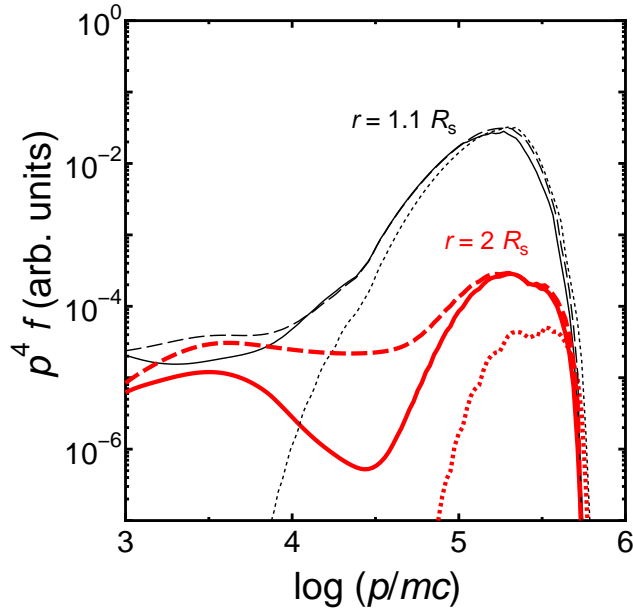


**Figure 3.** Spectra of CRs at  $r = 1.1 R_s$  and  $2 R_s$  at  $t = 10 t_0$ . Solid, dotted, and dashed lines are for Models A, B, and C, respectively.

#### 4 CONCLUSION

We have investigated the escape of CR protons accelerated at an SNR and their diffusion in the surrounding ISM. We solved a diffusion-convection equation from the vicinity of the shock front to the region far away from the front. We also considered the amplifications of Alfvén waves generated by the escaping CR particles, which affects the diffusion of the particles into the ambient ISM. We found that the amplification of the waves reduces the diffusion coefficient on a scale of the SNR and the escape of the particles is significantly delayed. Our results suggests that the particle scattering by the waves should have influence on the energy spectrum of CR particles observed at molecular clouds around SNRs in the  $\gamma$ -ray band.

#### ACKNOWLEDGMENTS

We thank T. Tsuribe for useful discussions. This work was supported by KAKENHI (Y. F.: 20540269; F. T.: 20540231, K. I.: 21-1979).

#### REFERENCES

- Abdo A. A., et al., 2009, ApJ, 706, L1  
 Abdo A. A., et al., 2010, ApJ, 712, 459  
 Abdo A. A., et al., 2010, ApJ, 718, 348  
 Abdo A. A., et al., 2010, Sci, 327, 1103  
 Aharonian F. A., et al., 2004, Natur, 432, 75  
 Aharonian F., et al., 2005, A&A, 437, L7  
 Aharonian F., et al., 2008, A&A, 481, 401  
 Bell A. R., 1978, MNRAS, 182, 147  
 Berezhko E. G., Yelshin V. K., Ksenofontov L. T., 1994, APh, 2, 215  
 Caprioli D., Blasi P., Amato E., 2009, MNRAS, 396, 2065

- O’C Drury L., Duffy P., Kirk J. G., 1996, A&A, 309, 1002  
 Fujita Y., Ohira Y., Takahara F., 2010, ApJ, 712, L153  
 Fujita Y., Ohira Y., Tanaka S. J., Takahara F., 2009, ApJ, 707, L179  
 Gabici S., Aharonian F. A., Casanova S., 2009, MNRAS, 396, 1629  
 Giuliani A., et al., 2010, A&A, 516, L11  
 Kawanaka N., Ioka K., Ohira Y., Kashiyama K., 2011, ApJ, 729, 93  
 Kulsrud R. M., Cesarsky C. J., 1971, ApL, 8, 189  
 Lee S.-H., Kamae T., Ellison D. C., 2008, ApJ, 686, 325  
 Lucek S. G., Bell A. R., 2000, MNRAS, 314, 65  
 Ohira Y., Murase K., Yamazaki R., 2010, A&A, 513, A17  
 Ohira Y., Murase K., Yamazaki R., 2011, MNRAS, 410, 1577  
 Ptuskin V. S., Zirakashvili V. N., 2003, A&A, 403, 1  
 Skilling J., 1975, MNRAS, 173, 255  
 Tavani M., et al., 2010, ApJ, 710, L151  
 Torres D. F., Rodriguez Marrero A. Y., de Cea Del Pozo E., 2008, MNRAS, 387, L59  
 Uchiyama Y., Blandford R. D., Funk S., Tajima H., Tanaka T., 2010, ApJ, 723, L122  
 Vladimirov A., Ellison D. C., Bykov A., 2006, ApJ, 652, 1246